JOURNAL OF MULTIDISCIPLINARY SCIENCES AND INNOVATIONS

VOLUME 5, ISSUE 03
MONTHLY JOURNALS

GERMAN INTERNATIONAL JOURNALS

ISSN NUMBER: 2751-4390
IMPACT FACTOR: 9,08

MATHEMATICAL MODELING IN DEFORMABLE SOLID MECHANICS: THEORY, FORMULAS, AND ANALYSIS

Rajabov Azamat

Department of Technological Machines and Information

Systems, Asia International University

ANNOTATION

This article presents a systematic description of the main mathematical models of deformable solid mechanics (DSM). The stress tensor, generalized Hooke's law, Euler–Bernoulli model, and failure criteria are provided along with analytical solutions. All formulas are numbered and accompanied by detailed explanations. Theoretical results are illustrated with graphs computed in Python/Matplotlib: stress–strain diagrams, beam deflection profiles, Kirsch stress contour fields, and failure surfaces. A comparative analysis table is provided for steel, aluminum, and CFRP materials.

Keywords

DSM, stress tensor, strain tensor, Hooke's law, beam deflection, Kirsch formula, Von Mises criterion, Tresca criterion, mathematical modeling

INTRODUCTION

Deformable solid mechanics (DSM) is a fundamental branch of mechanics that studies the deformation, stress state, and failure of solid bodies under the action of external forces, pressure, and temperature. This field provides the theoretical foundation for the reliable design of modern engineering devices and is applied to all types of structures, ranging from bridges, aircraft, reactors, and medical implants to nanoelements.

The mathematical framework of DSM is based on three main groups of equations: (1) equilibrium equations — the relationship between internal forces and external loads; (2) geometric relations — the connection between displacements and strains; (3) physical relations (Hooke's law) — the relationship between stress and strain. These three groups are combined to obtain the complete formulation of the elastic problem.

This article considers four main mathematical models: the generalized Hooke's law, the differential equation of beam bending, Kirsch stress concentration, and failure criteria. For each model, an analytical solution, a calculation example, and original graphical illustrations are provided.

STRESS AND STRAIN TENSORS

Stress Tensor

At an arbitrary point within an elastic body, the stress state is represented by the second-order symmetric tensor σ_{ij}. In the Cartesian coordinate system, the stress tensor has the following matrix form:

$$\sigma_{ij}=\begin{pmatrix}\sigma_{xx} & \tau_{xy} & \tau_{xz}\\ \tau_{yx} & \sigma_{yy} & \tau_{yz}\\ \tau_{zx} & \tau_{zy} & \sigma_{zz}\end{pmatrix} \qquad (1)$$

here:

- $\sigma_{xx},\sigma_{yy},\sigma_{zz}$— **Normal stresses**
- $\tau_{xy}=\tau_{yx},\ \tau_{yz}=\tau_{zy},\quad \tau_{zx}=\tau_{xz}$- Shear stresses (tensor symmetry).

Symmetry condition:

$$\sigma_{ij}=\sigma_{ji}$$

that is, in an elastic medium, the stress tensor is symmetric.

The symmetry of the tensor $(\tau_{ij}=\tau_{ji})$ follows from the equations of moment equilibrium. As a result, the number of independent components decreases from 9 to 6.

In index notation, the equilibrium equation is briefly written as follows:

$$\sigma_{ij,j}+F_i=0,(i=1,2,3) \qquad (2)$$

Here:

- F_i— Components of body forces
- The index following a comma denotes differentiation with respect to the coordinates.

2.2. Strain Tensor and Geometric Relations

In the theory of small deformations $\left(\frac{\partial u_i}{\partial x_j}\ll 1\right)$ the strain tensor ε_{ij}

$$\mathbf{u}=(u,v,w)$$

is defined through the first-order derivatives of the displacement vector:

$$\varepsilon_{xx}=\frac{\partial u}{\partial x},\varepsilon_{yy}=\frac{\partial v}{\partial y},\varepsilon_{zz}=\frac{\partial w}{\partial z} \qquad (3)$$

$$\gamma_{xy}=\frac{\partial u}{\partial y}+\frac{\partial v}{\partial x},\gamma_{yz}=\frac{\partial v}{\partial z}+\frac{\partial w}{\partial y},\gamma_{zx}=\frac{\partial w}{\partial x}+\frac{\partial u}{\partial z} \qquad (4)$$

here:

- ε_{ii}—inear (normal) strains;
- $\gamma_{ij}=2\varepsilon_{ij}$—angular (shear) strains.

GENERALIZED HOOKE'S LAW

Complete Expression for Isotropic Material

For a linearly elastic isotropic material, the relationship between stress and strain (generalized Hooke's law) is expressed as:

Two independent elastic constants — E (Young's modulus) and **ν** (Poisson's ratio) — define all material properties:

$$\varepsilon_{xx} = \frac{1}{E}[\sigma_{xx} - \nu(\sigma_{yy} + \sigma_{zz})] \quad (5)$$

$$\varepsilon_{yy} = \frac{1}{E}[\sigma_{yy} - \nu(\sigma_{xx} + \sigma_{zz})] \quad (6)$$

$$\varepsilon_{zz} = \frac{1}{E}[\sigma_{zz} - \nu(\sigma_{xx} + \sigma_{yy})] \quad (7)$$

$$\gamma_{xy} = \frac{\tau_{xy}}{G}, \gamma_{yz} = \frac{\tau_{yz}}{G}, \gamma_{zx} = \frac{\tau_{zx}}{G} \quad (8)$$

The shear modulus G expressed through E and ν:

$$G = \frac{E}{2(1+\nu)}$$

Example (steel):

$$E = 210 \text{ GPa}, \nu = 0.30 \Rightarrow G = 80.8 \text{ GPa}$$

In matrix form:

$$\{\sigma\} = [C] \cdot \{\varepsilon\} \text{ yoki } \{\varepsilon\} = [S] \cdot \{\sigma\} \quad (9)$$

here:

[C] — stiffness matrix

$[S] = [C]^{-1}$— compliance matrix

3.2. Stress–Strain Diagram

The stress–strain (σ–ε) diagram is the most important graphical tool for describing the mechanical properties of a material. Figure 1 shows the diagrams for three different materials. For steel, a bilinear elastic–plastic model is used: in the elastic region, E = 210 GPa; in the plastic region, the tangent modulus E_t = 8 GPa.

JOURNAL OF MULTIDISCIPLINARY SCIENCES AND INNOVATIONS

VOLUME 5, ISSUE 03
MONTHLY JOURNALS

ISSN NUMBER: 2751-4390
IMPACT FACTOR: 9,08

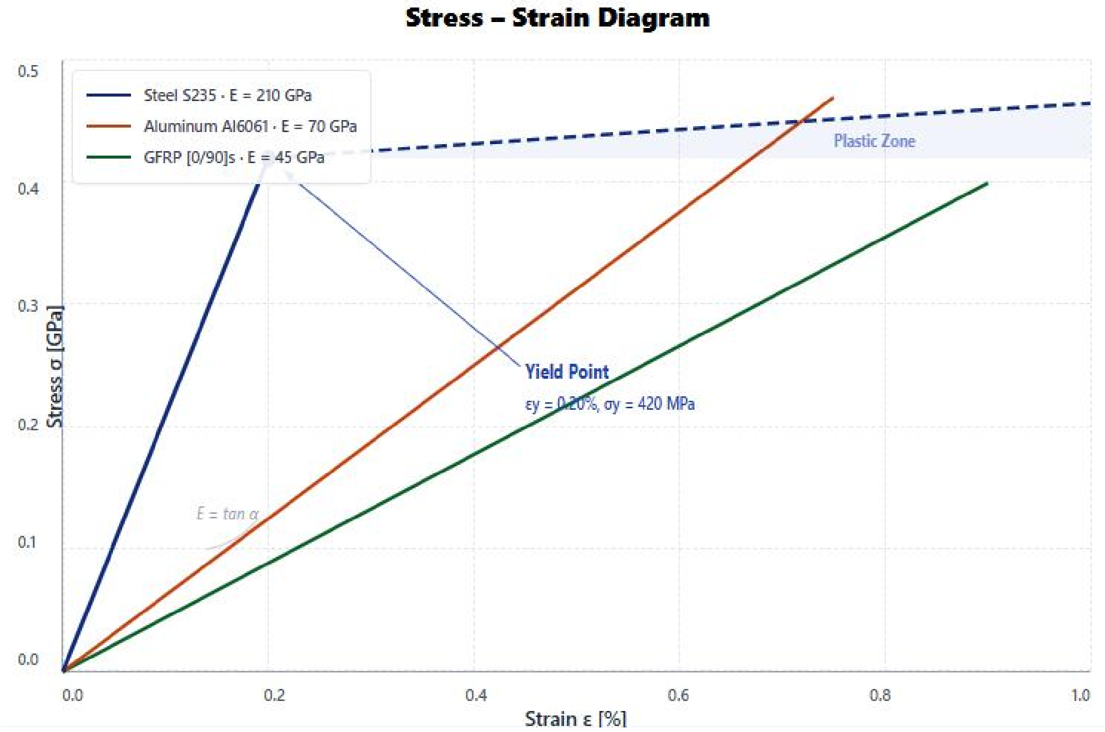

Figure 1. Stress–strain diagram: Steel S235 (blue), Aluminum Al6061 (dark orange), GFRP [0/90]s (green). Yield point for steel: ε_y=0.20%,σ_y=420 *MPa*

As seen in Figure 1, the three materials exhibit significant differences in Young's modulus:

$$E_{\text{steel}}=210\text{ GPa},E_{\text{Al}}=70\text{ GPa},E_{\text{GFRP}}=45\text{ GPa}$$

Steel is distinguished by its deformability in the plastic region, whereas GFRP exhibits linear elastic behavior throughout the entire loading.

4. BEAM BENDING: DIFFERENTIAL MODEL

4.1. Euler–Bernoulli fourth-order equation

The small deflection of a cantilever beam is described, according to Euler–Bernoulli theory, by the following fourth-order differential equation:

$$EI\frac{d^4w}{dx^4}=q(x) \quad (10)$$

here:

- E— Young's modulus [MPa]
- I— moment of inertia of the cross-section [m⁴]
- $w(x)$— deflection [m]
- $q(x)$— distributed load intensity [N/m]

Boundary conditions for a cantilever beam fixed at one end (x = 0) and free at the other end (x = L):

Fixed end (x = 0 — no displacement and no rotation):

$$w(0)=0,\ \frac{dw}{dx}|_{x=0}=0 \quad (11)$$

Free end (x = L — no bending moment and no shear force):

$$\frac{d^2w}{dx^2}|_{x=L}=0, \frac{d^3w}{dx^3}|_{x=L}=0 \quad (12)$$

Analytical Solution and Profiles

For a uniformly distributed load q = "const", the complete analytical solution of equation (10) is obtained by integrating it four times and applying the boundary conditions (11)–(12):

$$w(x)=\frac{q}{24EI}(x^4-4Lx^3+6L^2x^2)(13)$$

$$M(x)=EI\frac{d^2w}{dx^2}=\frac{q}{2}(L-x)^2(14)$$

$$V(x)=EI\frac{d^3w}{dx^3}=q(L-x)(15)$$

Maximum values:

- **Maximum deflection at the free end:** $w_{\max}=\frac{qL^4}{8EI}$
- **Maximum moment at the fixed end:** $M_{\max}=\frac{qL^2}{2}$

Example:

$$q=10\text{ kN/m},\ L=1\text{ m}, EI=500\text{ kN\cdotpm}^2$$
$$w_{\max}=2.50\text{ mm},\ M_{\max}=5.00\text{ kN\cdotpm}$$
$$V_{\max}=10.00\text{ kN}$$

***Figure 2** shows the profiles of deflection, bending moment, and shear force.*

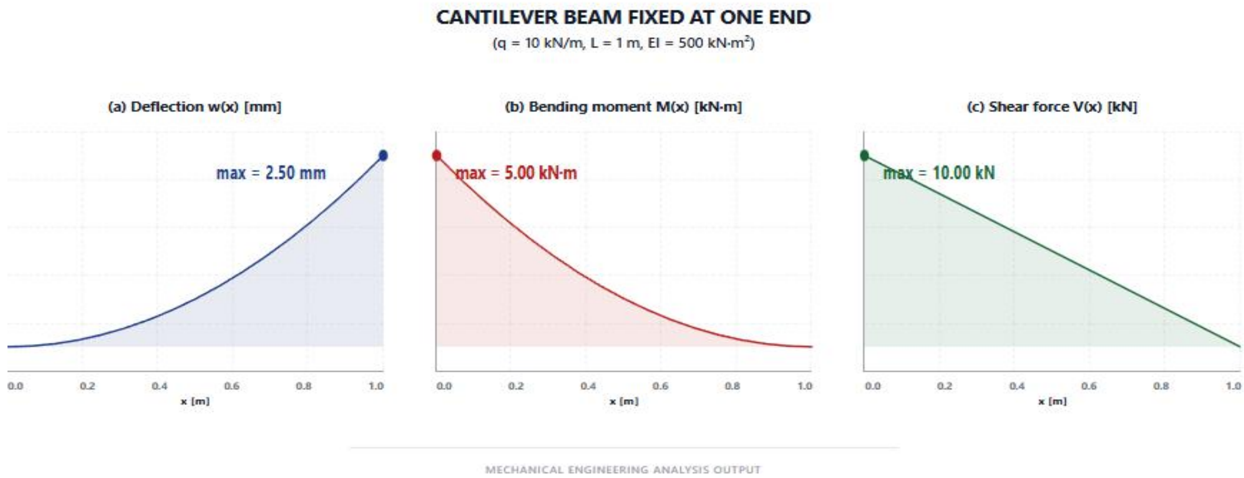

Figure 2. Cantilever beam:

Figure 2. Cantilever beam (q = 10 kN/m, L = 1 m, EI = 500 kN·m²): (a) deflection w(x) [mm]; (b) bending moment M(x) [kN·m]; (c) shear force V(x) [kN]. Maximum values are indicated by dark points.

STRESS CONCENTRATION IN A PLATE WITH A HOLE

Kirsch Analytical Solution For an infinite plate with a circular hole of radius $a$subjected to a uniaxial far-field stress σ_∞, the complete stress field in polar coordinates $(r\theta)$ was exactly solved by Kirsch (1898):

$$\sigma_{rr}=\frac{\sigma_\infty}{2}\left(1-\frac{a^2}{r^2}\right)+\frac{\sigma_\infty}{2}\left(1-\frac{4a^2}{r^2}+\frac{3a^4}{r^4}\right)\cos 2\theta \quad (16)$$

$$\sigma_{\theta\theta}=\frac{\sigma_\infty}{2}\left(1+\frac{a^2}{r^2}\right)-\frac{\sigma_\infty}{2}\left(1+\frac{3a^4}{r^4}\right)\cos 2\theta \quad (17)$$

$$\tau_{r\theta}=-\frac{\sigma_\infty}{2}\left(1+\frac{2a^2}{r^2}-\frac{3a^4}{r^4}\right)\sin 2\theta \quad (18)$$

here:

a — hole radius

r — distance from the center **(r ≥ a)**

θ — angle

5.2. Stress Concentration Factor

At the edge of the hole (r = a) and θ = 90°, the tangential stress σ_θθ reaches its maximum value. From equation (17):

$$\sigma_{\theta\theta}|_{r=a,\,\theta=90^\circ}=3\sigma_\infty \quad (19)$$

The stress concentration factor (SCF) is the ratio of the maximum stress to the nominal far-field stress:

$$K_t = \frac{\sigma_{max}}{\sigma_\infty} = 3 \quad (20)$$

he value $K_t=3$does not depend on the material type, load magnitude, or hole radius — it is a universal indicator determined only by the geometric shape.

If $\sigma_\infty=100\text{MPa}$:

- At the edge of the hole, $\sigma_{\theta\theta}=300\text{MPa}$
- At $r=2a$, it drops to approximately 122 MPa

This demonstrates the rapid decay of stress away from the hole. Figure 3 shows the contour field and radial distribution graph.

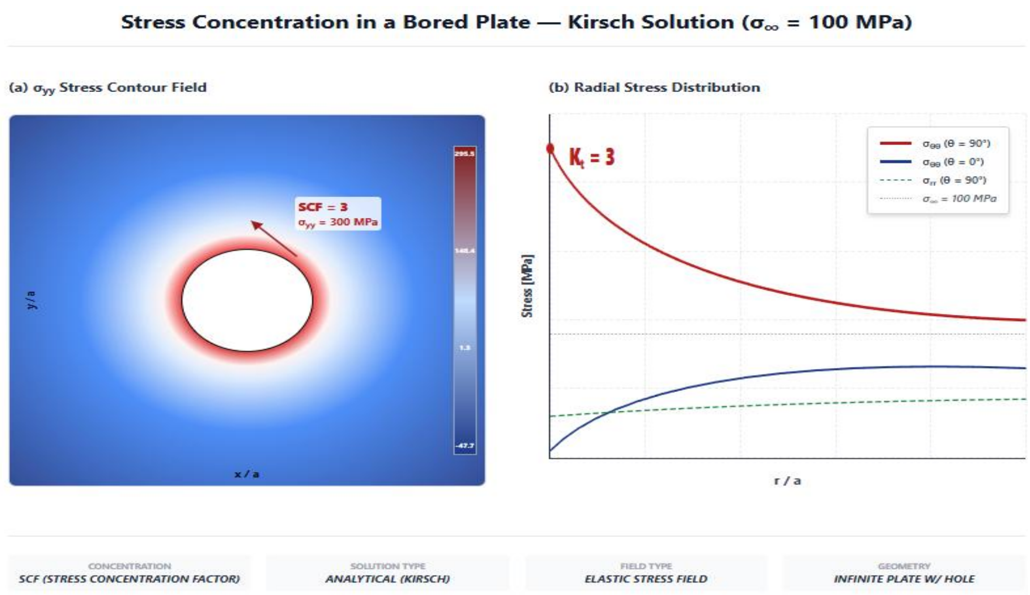

Figure 3. Kirsch stress distribution ($\sigma\infty$ = *100 MPa, a = 1 m*): (a) σ_{yy} stress contour field — maximum 300 MPa at the hole edge (K_t = 3); (b) variation of stress versus r/a along θ = 90° and 0° directions.

FAILURE CRITERIA: VON MISES AND TRESCA

Von Mises Plastic Yield Criterion

Determining the onset of plastic yielding under a complex stress state is an important engineering problem. The Von Mises (1913) criterion is based on the concept of distortion energy: yielding begins when the octahedral shear stress reaches a critical value:

$$\sigma_{VM} = \sqrt{\frac{(\sigma_1-\sigma_2)^2+(\sigma_2-\sigma_3)^2+(\sigma_3-\sigma_1)^2}{2}} \geq \sigma_y \qquad (21)$$

Here, $\sigma_1\geq\sigma_2\geq\sigma_3$are the principal stresses, and $\sigma_y$is the yield stress obtained from a uniaxial test.

JOURNAL OF MULTIDISCIPLINARY SCIENCES AND INNOVATIONS
VOLUME 5, ISSUE 03
MONTHLY JOURNALS
ISSN NUMBER: 2751-4390
IMPACT FACTOR: 9,08

In a plane stress state (σ_3=0), the Von Mises criterion forms an ellipse in the $\sigma_1-\sigma_2$ plane. In pure shear ($\sigma_1=-\sigma_2=\tau$):

$$\tau_{VM}=\frac{\sigma_y}{\sqrt{3}}\approx 0.577\cdot\sigma_y \qquad (22)$$

Tresca Plastic Yield Criterion

The Tresca (1864) criterion is based on the maximum shear stress: yielding begins when the maximum shear stress reaches a critical value:

$$\tau_{\max}=\frac{\sigma_1-\sigma_3}{2}\geq\frac{\sigma_y}{2} \qquad (23)$$

In pure shear, the Tresca criterion gives:

$$\tau_{\text{Tresca}}=\frac{\sigma_y}{2}=0.500\cdot\sigma_y.$$

The greatest difference between the Von Mises and Tresca criteria occurs in pure shear: from (22) and (23), $0.577/0.500=15.5\%$. The Von Mises criterion provides results closer to experimental data, while Tresca is more conservative (safer). Figure 4 shows the graphical representation of both criteria in the $\sigma_1-\sigma_2$ plane.

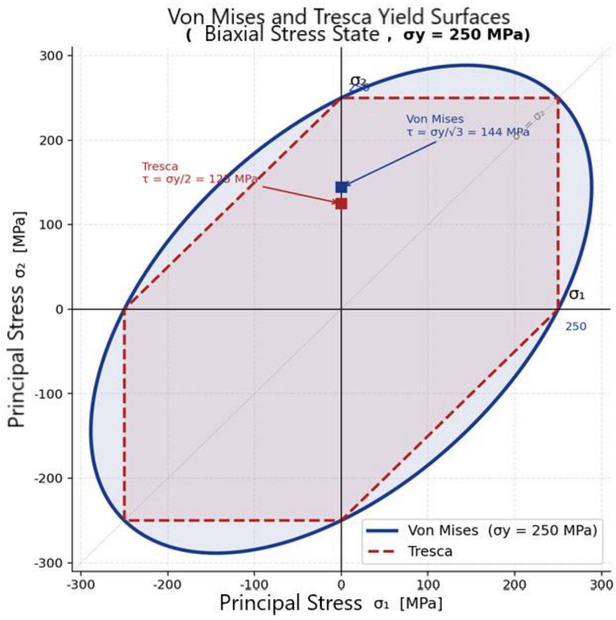

Figure 4. Von Mises (blue ellipse) and Tresca (red hexagon) yield surfaces, σy = 250 MPa. Shaded areas: inner — elastic region, outer — plastic yielding. The 15.5% difference between the two criteria in pure shear points is clearly visible.

MECHANICAL PROPERTIES OF MATERIALS: COMPARATIVE TABLE

Table 1 presents the main mechanical properties of the materials used in the mathematical models discussed in the article. All values are taken from standard material catalogs.

Table 1. Mechanical Properties of Key Construction Materials

Material	E (GPa)	σy (MPa)	σu (MPa)	ρ (kg/m³)	Main Application
Steel S235	210	235	400	7 850	Civil engineering structures
Steel S355	210	355	510	7 850	Bridges, cranes
Aluminum Al6061	70	270	310	2 700	Aerospace, transport
GFRP [0/90]s	45	280	400	1 800	Construction, marine
CFRP [0/90]s	120	600	900	1 600	*Aerospace, sports*
Copper Cu	120	200	250	8 960	*Electrical engineering*

As seen from the table, CFRP combines the highest strength with the lowest density, offering a comparative strength 18 times greater than steel. However, due to its high cost, steel S235/S355 remains predominant in mass construction. Aluminum provides an optimal balance for the aerospace sector: low weight combined with sufficient strength.

8. RESULTS AND DISCUSSION

The four mathematical models presented in the article cover the most important aspects of DSM and are logically interconnected:

- **Hooke's law (5)–(9)** provides the physical description of the material and serves as the basis for all other models. The elastic modulus $E$and Poisson's ratio $\nu$are the input parameters for any linear elastic problem.

- **Beam equation (10)–(15)** combines Hooke's law with bending kinematics. The analytical solution (13) allows obtaining deflection, bending moment, and shear force within a single differential model: for q=10 kN/m, L=1 m, $w_{\max}$=2.50 mm, $M_{\max}$=5.00 kN\cdotpm.

- **Kirsch formulas (16)–(20)** provide an exact description of stress concentration in a plate with a hole. The value K_t=3serves as a universal indicator widely used in engineering design to identify hazardous zones around holes. The stress decreases from σ_∞·3.0at r=$a$to approximately 1.07σ_∞at r=3a.

- **Von Mises and Tresca criteria (21)–(23)** predict when a material exits the elastic range. In pure shear, the difference is 15.5%: Von Mises is closer to experimental results, while Tresca provides a more conservative estimate for engineering design.

Important limitation: All analytical solutions are based on the assumption that the material is linearly elastic, isotropic, and homogeneous. Since composite materials (GFRP, CFRP) are anisotropic, these models can only be used as a macro-level approximation. For complex geometries and boundary conditions, the finite element method (FEM) is required.

CONCLUSION

1. The mathematical framework of DSM is based on three main groups of equations — equilibrium (2), geometric (3)–(4), and physical (5)–(8) — whose combination provides the complete formulation of the elastic problem.

2. The analytical solution obtained from the Euler–Bernoulli differential equation (10) (equations 13–15) provides deflection, bending moment, and shear force within a single model for a cantilever beam: for q=10 kN/m, L=1 m, $w_{\max}$=2.50 mm, $M_{\max}$=5.00 kN\cdotpm.

3. The Kirsch formulas (16)–(17) show that the stress concentration factor around a hole is $K_t=3$. For $\sigma_\infty=100$ MPa, this corresponds to a stress of 300 MPa at the hole edge — a critical zone requiring attention in engineering design.

4. The Von Mises and Tresca criteria complement each other: in pure shear, $\tau_{\mathrm{VM}}=0.577\sigma_y$ and $\tau_{\mathrm{Tresca}}=0.500\sigma_y$. For high-safety structures, the Tresca criterion is recommended.

5. The four original figures (Figures 1–4) visually confirm the theoretical results and significantly facilitate the understanding of the physical meaning of the mathematical models.